An Arbitrary-Order Discontinuous Skeletal Method for Solving Electrostatics on General Polyhedral Meshes

Daniele A. Di Pietro[1], Bernard Kapidani[2], Ruben Specogna[2], and Francesco Trevisan[2]

[1]Institut Montpelliérain Alexander Grothendieck, University of Montpellier, 34095 Montpellier, France
[2]Polytechnic Department of Engineering and Architecture, Università di Udine, 33100 Udine, Italy

We present a numerical method named mixed high order (MHO) to obtain high order of convergence for electrostatic problems solved on general polyhedral meshes. The method, based on high-order local reconstructions of differential operators from face and cell degrees of freedom, exhibits a moderate computational cost thanks to hybridization and static condensation that eliminate cell unknowns. After surveying the method, we assess its effectiveness for 3-D problems by comparing, for the first time in literature, its performances with classical conforming finite elements. Moreover, we emphasize the algebraic equivalence of MHO in the lowest order with the analog formulation obtained with the discrete geometric approach or the finite-integration technique.

Index Terms—**Electrostatics, high order, Poisson problem, polyhedral meshes.**

I. Introduction

In THE past few years, the interest in discretization methods for diffusive problems on general polyhedral meshes has considerably grown (see, e.g., [1] and the references therein). Polyhedral mesh generators are currently being developed and, once available, will provide more flexibility in element shapes. This flexibility, in turn, should yield to easier techniques for adaptive mesh refinement, derefinement, and non-overlapping domain decomposition with non-matching grids. In particular, the non-conforming-like refinement—as the subgridding proposed in [2]—and the adaptive coarsening strategy [3] are particularly appealing.

We consider the problem of seeking the electric displacement vector field $d : \Omega \to \mathbb{R}^3$ and the scalar potential field $v : \Omega \to \mathbb{R}$ in a polyhedral domain $\Omega \subset \mathbb{R}^3$, such that

$$\varepsilon^{-1} d + \nabla v = 0 \quad \text{in } \Omega \tag{1a}$$

$$\varepsilon d = \rho_s \quad \text{in } \Omega \tag{1b}$$

$$v = 0 \quad \text{on } \partial\Omega \tag{1c}$$

where ρ_s is the volumetric source charge density and ε is the electric permittivity. We assume that ε is a constant on each element T of a polyhedral mesh $\mathcal{T}_h$ of the domain Ω, and we denote its value by ε_T.

This paper presents the mixed high-order (MHO) method of [4] (to which we refer to for all theoretical details and proofs), which is able to obtain high-order convergence in the solution of (1) on arbitrary polyhedral meshes. This paper aims at assessing its performance in terms of accuracy versus computational time on 3-D problems by comparison with classical conforming finite elements, for the first time in literature. This paper also emphasizes the analogies of the presented method with the discrete geometric approach (DGA) [2], in the lowest order case corresponding to the polynomial degree $k = 0$. In particular, this novel method is algebraically equivalent (up to the choice of a scalar parameter in the stabilisation term) to the mixed-hybrid geometric formulation described in [5]. The MHO method also bears some similarities with discontinuous Galerkin (DG) approaches [6], but presents a higher convergence rate for a given polynomial degree. However, contrary to DG, the degrees of freedom (DOFs) are attached to both faces and elements of the mesh. As shown below, cell-based unknowns may be easily eliminated by element-wise static condensation.

This paper is organized as follows. In Section II, we survey the MHO method and show how to reinterpret the DGA as the MHO method in the lowest order. Section III presents the comparison of results provided by the MHO with respect to finite elements on a test case for which an analytical solution is available. Finally, in Section IV, some conclusions are drawn.

II. The Mixed High-Order Method

The starting point of the MHO method is the classical weak formulation of problem (1): find $(d, v) \in D \times V$, such that for all $(\tau, u) \in D \times V$

$$\int_\Omega \varepsilon^{-1} d \cdot \tau - \int_\Omega v(\varepsilon\tau) = 0 \tag{2a}$$

$$\int_\Omega (\varepsilon d) u = \int_\Omega \rho_s u \tag{2b}$$

where D denotes the space of square-integrable vector-valued functions whose divergence is also square integrable, while V contains square-integrable scalar-valued functions. The main idea is to define some DOFs in each element to be able to locally reconstruct the divergence operator and the displacement d. These reconstructions are used to write discrete counterparts of each term of (2).

Let a polynomial degree $k \in \mathbb{N}$ be fixed, and consider a mesh element $T \in \mathcal{T}_h$. The local space of DOFs for the displacement is defined as the following polynomials (see Fig. 1):

$$\underline{D}_T^k := (\varepsilon_T \nabla \mathbb{P}^k(T)) \times \mathbb{P}^k(\mathcal{F}_T)$$

Manuscript received November 18, 2016; revised February 7, 2017; accepted February 7, 2017. Date of publication February 8, 2017; date of current version May 26, 2017. Corresponding author: R. Specogna (e-mail: ruben.specogna@uniud.it).

Color versions of one or more of the figures in this paper are available online at http://ieeexplore.ieee.org.

Digital Object Identifier 10.1109/TMAG.2017.2666546

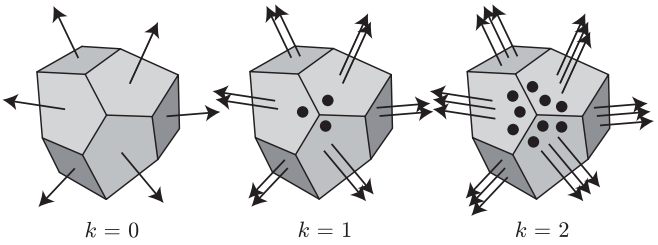

Fig. 1. Local DOFs in $\underline{D}_T^k$ for $k \in \{0, 1, 2\}$.

where $\mathbb{P}^k(\mathcal{F}_T)$ is the space of polynomials of degree k over the boundary of T that are possibly discontinuous at the edges shared by the faces of T. Element-based and face-based DOFs represent, respectively, polynomial moments of d inside T (which are vector-valued quantities) and polynomial moments of the outward normal component of d on F (which are scalars). We remark that element-based DOFs are present only for $k \geq 1$. For the collection of all DOFs in $\underline{D}_T^k$, we use the underlined notation $\underline{\tau}_T = (\tau_T, \tau_{\partial T})$, where τ_T contains the vector-valued element-based DOFs, while $\tau_{\partial T}$ contains the scalar-valued face-based DOFs.

We define the discrete divergence operator $\mathcal{D}_T^k : \underline{D}_T^k \to \mathbb{P}^k(T)$, such that for all $\underline{\tau}_T \in \underline{D}_T^k$ and all $q \in \mathbb{P}^k(T)$

$$\int_T (\mathcal{D}_T^k \underline{\tau}_T) q = -\int_T \tau_T \cdot \nabla q + \int_{\partial T} \tau_{\partial T} q. \tag{3}$$

Equation (3) resembles an integration by parts formula, where the role of the displacement inside T and on its boundary ∂T is played by τ_T and $\tau_{\partial T}$, respectively.

By similar principles, the displacement reconstruction operator $\mathcal{R}_T^k : \underline{D}_T^k \to \varepsilon_T \nabla \mathbb{P}^{k+1}(T)$ is such that for all $\underline{\tau}_T \in \underline{D}_T^k$ and all $w \in \mathbb{P}^{k+1}(T)$

$$\int_T \mathcal{R}_T^k \underline{\tau}_T \cdot \nabla w = -\int_T (\mathcal{D}_T^k \underline{\tau}_T) w + \int_{\partial T} \tau_{\partial T} w.$$

Notice that, for all $\underline{\tau}_T[T]$, $\mathcal{R}_T^k \underline{\tau}_T[T]$ is a polynomial one degree higher than the element-based DOFs τ_T.

For all $T \in \mathcal{T}_h$, the local contribution $\int_T \varepsilon^{-1} d \cdot \tau$ to the first term in (2a) is approximated by the bilinear form m_T on $\underline{D}_T^k \times \underline{D}_T^k$, such that

$$m_T(\underline{d}_T, \underline{\tau}_T) := \int_T \varepsilon_T^{-1} \mathcal{R}_T^k \underline{d}_T \cdot \mathcal{R}_T^k \underline{\tau}_T + s_{\Sigma,T}(\underline{d}_T, \underline{\tau}_T)$$

with stabilization bilinear form given by

$$s_{\Sigma,T}(\underline{d}_T, \underline{\tau}_T) := \int_{\partial T} \gamma_{\partial T} (\mathcal{R}_T^k \underline{d}_T \cdot n_{\partial T} - d_{\partial T})(\mathcal{R}_T^k \underline{\tau}_T \cdot n_{\partial T} - \tau_{\partial T}) \tag{4}$$

where $n_{\partial T}$ is the vector field representing the face normals on ∂T pointing out of T and

$$\gamma_{\partial T} := h_T (\varepsilon_T n_{\partial T} \cdot n_{\partial T})^{-1} \tag{5}$$

with h_T diameter of T. This stabilization is mandatory for the bilinear form m_T to be symmetric positive-definite (SPD). The idea behind (4) is to penalize in a least-square sense, the difference between two quantities that both represent the normal component of the displacement on ∂T.

We next introduce the global space $\underline{\check{D}}_h^k$ of fully discontinuous DOFs for the displacement as well as its subspace $\underline{D}_h^k$ with continuous face-based DOFs

$$\underline{\check{D}}_h^k := \times_{T \in \mathcal{T}_h} \underline{D}_T^k$$
$$\underline{D}_h^k := \big\{ \underline{\tau}_h \in \underline{\check{D}}_h^k \mid \forall F \in \mathcal{F}_{T1} \cap \mathcal{F}_{T2},\ \tau_{\partial T_1 | F} + \tau_{\partial T_2 | F} = 0 \big\}.$$

In practice, this is easily achieved in the usual assembling process by considering the same DOFs for the face shared by two elements.

The approximation of the scalar potential v is sought in

$$V_h^k := \mathbb{P}^k(\mathcal{T}_h).$$

The MHO method reads: find $(\underline{d}_h, v_h) \in \underline{D}_h^k \times V_h^k$, such that for all $(\underline{\tau}_h, u_h) \in \underline{D}_h^k \times V_h^k$, it holds

$$m_h(\underline{d}_h, \underline{\tau}_h) - \int_\Omega (D_h^k \underline{\tau}_h) v_h = 0 \tag{6a}$$
$$\int_\Omega (D_h^k \underline{d}_h) u_h = \int_\Omega \rho_s u_h \tag{6b}$$

where m_h is obtained by the usual element-by-element assembly and D_h^k is set equal to $\mathcal{D}_T^k$ applied to the restriction of $\underline{\tau}_h$ inside each element $T \in \mathcal{T}_h$. Convergence as h^{k+1} for the displacement and as h^{k+2} for the potential is proved in [4].

A. Hybridization to Obtain an SPD System Matrix

In Section III, we use a reformulation of (6) to obtain an SPD sparse system matrix (on the contrary, (6) is a saddle-point problem). At the continuous level, the idea is to eliminate the displacement d in (1) and consider the following classical primal formulation, where the potential v is the only unknown: find $v \in U$, such that for all $u \in U$

$$a(v, u) := \int_\Omega \varepsilon \nabla v \cdot \nabla u = \int_\Omega \rho_s u \tag{7}$$

where U contains square-integrable, finite-energy functions, which comply with the boundary condition (1c).

At the discrete level, the local elimination of the displacement is performed by enforcing the continuity of the interface DOFs in $\underline{D}_h^k$ by Lagrange multipliers (which can be interpreted as in [5] as traces of the potential) and inverting, inside each element $T \in \mathcal{T}_h$, the local constitutive laws expressed by (6a) (see, e.g., [7] for details).

Let us introduce the following space of hybrid DOFs:

$$\underline{V}_h^k := V_h^k \times \mathbb{P}^k(\mathcal{F}_h).$$

For a generic element of $\underline{V}_h^k$, we use the underlined notation $\underline{v}_h = (v_h, (v_F)_{F \in \mathcal{F}_h})$. The discrete counterpart of v regarded as an element of U is sought in the subspace $\underline{V}_{h,0}^k$ of $\underline{V}_h^k$, incorporating the homogeneous Dirichlet condition on $\partial\Omega$

$$\underline{V}_{h,0}^k := \big\{ \underline{v}_h \in \underline{V}_h^k \mid v_F = 0 \quad \forall F \in \partial\Omega \big\}.$$

Let us again concentrate on one element $T \in \mathcal{T}_h$. We denote by $\underline{V}_T^k$ the restriction of $\underline{V}_h^k$ to T and, for all $\underline{v}_T \in \underline{V}_T^k$, we let $v_{\partial T}$ be the broken polynomial function on ∂T, such that $v_{\partial T | F} = v_F$ for all $F \in \mathcal{F}_T$, so that $\underline{v}_T = (v_T, v_{\partial T})$

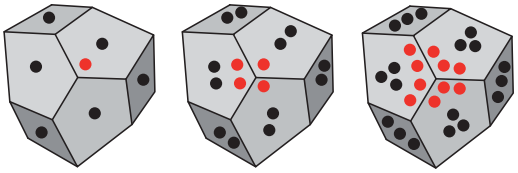

Fig. 2. Local DOFs in $\underline{V}_T^k$ for $k \in \{0, 1, 2\}$. DOFs represented by red dots can be eliminated locally by the static condensation procedure described in [7].

(see Fig. 2). From the potential DOFs in $\underline{V}_T^k$, we can define a reconstruction of displacement DOFs in $\underline{D}_T^k$ through the potential-to-displacement mapping operator $\underline{\varsigma}_T^k : \underline{V}_T^k \to \underline{D}_T^k$, such that for all $\underline{v}_T \in \underline{V}_T^k$ and all $\underline{\tau}_T \in \underline{D}_T^k$

$$m_T\left(\underline{\varsigma}_T^k \underline{v}_T, \underline{\tau}_T\right) = -\int_T v_T \left(\mathcal{D}_T^k \underline{\tau}_T\right) + \int_{\partial T} v_{\partial T}\, \tau_{\partial T}.$$

A high-order reconstruction of the potential can, then, be defined through the operator $p_T^{k+1} : \underline{V}_T^k \to \mathbb{P}^{k+1}(T)$, such that for all $\underline{v}_T \in \underline{V}_T^k$

$$-\varepsilon_T \nabla p_T^{k+1} \underline{v}_T = \mathcal{R}_T^k\left(\underline{\varsigma}_T^k \underline{v}_T\right), \quad \int_T \left(p_T^{k+1} \underline{v}_T - v_T\right) = 0.$$

For a given $\underline{v}_T \in \underline{V}_T^k$, $p_T^{k+1} \underline{v}_T$ is a polynomial one degree higher than the element-based DOFs v_T. $p_T^{k+1} \underline{v}_T$ can be computed directly from the hybrid DOFs in $\underline{v}_T$, solving the following problem: for all $w \in \mathbb{P}^{k+1}(T)$

$$\int_T \varepsilon_T \nabla p_T^{k+1} \underline{v}_T \cdot \nabla w = \int_T \varepsilon_T \nabla v_T \cdot \nabla w + \int_{\partial T} \left(v_{\partial T} - v_T\right) \varepsilon_T \nabla w \cdot n_{\partial T}.$$

Consider the following approximation of (7): find $(\underline{d}_h, \underline{v}_h) \in \underline{\check{D}}_h^k \times \underline{V}_{h,0}^k$, such that for all $T \in \mathcal{T}_h$

$$\underline{d}_T = -\underline{\varsigma}_T^k \underline{v}_T \tag{8a}$$

and, for all $\underline{u}_h \in \underline{V}_{h,0}^k$

$$a_h(\underline{v}_h, \underline{u}_h) := \sum_{T \in \mathcal{T}_h} a_T(\underline{v}_T, \underline{u}_T) = \int_\Omega \rho_s u_h \tag{8b}$$

where the local bilinear form a_T on $\underline{V}_T^k \times \underline{V}_T^k$ is

$$a_T(\underline{v}_T, \underline{u}_T) := \int_\Omega \varepsilon_T \nabla p_T^{k+1} \underline{v}_T \cdot \nabla p_T^{k+1} \underline{u}_T + s_{\Sigma,T}\left(\underline{\varsigma}_T^k \underline{v}_T, \underline{\varsigma}_T^k \underline{u}_T\right).$$

It can be proved that $\underline{d}_h \in \underline{D}_h^k$ and, with $v_h \in V_h^k$ the broken polynomial function obtained from element-based DOFs in $\underline{v}_h$, $(\underline{d}_h, v_h) \in \underline{D}_h^k \times V_h^k$ solves (6).

B. Link With DGA or Finite-Integration Technique

The DGA of [2] is equivalent to the MHO formulation (6) in the lowest order case (i.e., $k = 0$). For the equivalence to work, we first have to assume that, for every mesh element $T \in \mathcal{T}_h$, there exists a point x_T (i.e., the dual node $\tilde{n}$) with respect to which T is star-shaped.

The only difference between the two approaches is in the stabilization parameter $\gamma_{\partial T}$ which, in the case of DGA, is such that for all $F \in \mathcal{F}_T$ [compare with (5)]

$$\gamma_{\partial T}^{\mathrm{dga}}{}_{|F} = (3\,\mathrm{dist}(x_T, F))^{-1} \varepsilon_T^{-1} (x_F - x_T) \cdot (x_F - x_T)$$

where x_F denotes the barycenter of F.

III. Numerical Results

The implementation of the proposed method is based on the primal form (8). The size of the linear system to be solved is further reduced by locally eliminating element-based DOFs by static condensation (represented in red in Fig. 2) (see [7] for details). Therefore, accounting for the strong enforcement of Dirichlet boundary conditions, a matrix of size $N_{\mathrm{dof}} \times N_{\mathrm{dof}}$ is obtained, where $N_{\mathrm{dof}} = \mathrm{card}(\mathcal{F}_h^{\mathrm{i}}) \times \binom{k+2}{k}$ and $\mathrm{card}(\mathcal{F}_h^{\mathrm{i}})$ is the number of faces in the interior of $\mathcal{T}_h$. We use a scaled monomials basis for the space of discontinuous polynomials (see [7] for implementation details with such basic functions).

The performance of the method is assessed on a problem for which an analytical solution is available (other tests presenting singularities may be found in [3]): we consider an electrostatic problem in the unit cube $\Omega = (0, 1)^3$ subject to homogeneous Dirichlet boundary conditions. The charge density ρ_s is selected so that the exact solution is $v = \sin(\pi\, x)\, \sin(\pi\, y)\, \sin(\pi\, z)$. We evaluate the performances of MHO for polynomial orders $0 \le k \le 4$ by solving the problem on five isotropic tetrahedral meshes obtained as the refinement of the coarsest one. All the sparse linear systems are solved with the algebraic multigrid solver AGMG [8] by stopping the iterations once the relative residual reaches 1×10^{-9}. The computations are performed on a laptop equipped with an Intel Core i7-3720QM 2.6 GHz processor with 16 GB of RAM.

We consider, as a first error measure, the error in the energy norm defined as $e_{\mathrm{en}} := \|\varepsilon^{1/2} \nabla h(v - \mathcal{P}_h^{k+1} \underline{v}_h)\|$, where v denotes the exact solution and $\mathcal{P}_h^{k+1}$ is equal to p_T^{k+1} applied to the restriction of $\underline{v}_h$ for all $T \in \mathcal{T}_h$. We also monitor the approximation of the electrostatic energy $E := (1/(2))\, a(v, v) - \int_\Omega \rho_s v$ defined as $E_h := (1/(2))\, a_h(\underline{v}_h, \underline{v}_h) - \int_\Omega \rho_s v_h$. Since most global quantities of interest, such as the capacitance, may be obtained from energy, this second error measure is very important in electromagnetic applications.

We remark that we also include measures of the computational time, defined as the total wall time needed for the simulation (i.e., not just CPU time), including the preprocessing (mesh generation and creation of mesh incidences), the assembly of the sparse matrix, the solution of the linear system, and the postprocessing (electrostatic energy; energy error; and, above all, data storage for visualization).

Figs. 3 and 4 show the convergence in energy norm e_{en} with respect to the mesh density h and the number of DOFs N_{dof}, respectively. As expected, the asymptotic convergence of e_{en} with respect to h coincides with the one predicted by theory. Fig. 5 shows the convergence of the difference between the total electrostatic energy E and the estimated one E_h with respect to the computational time required. From Fig. 5, we can conclude that the method is convenient even if one is

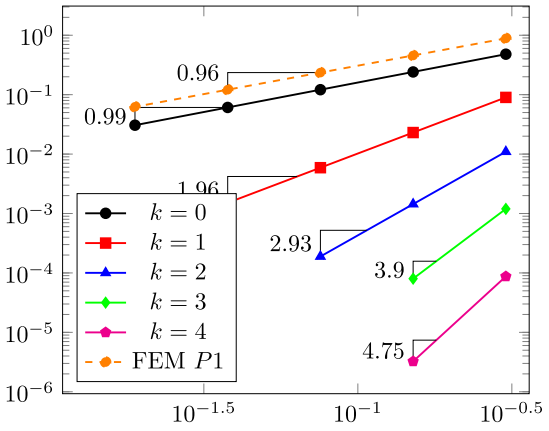

Fig. 3. e_{en} versus h.

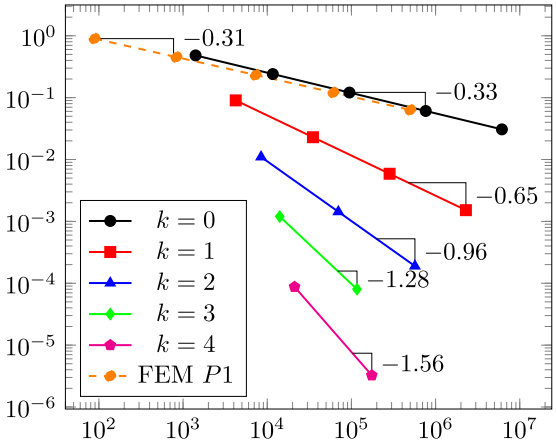

Fig. 4. e_{en} versus N_{dof}.

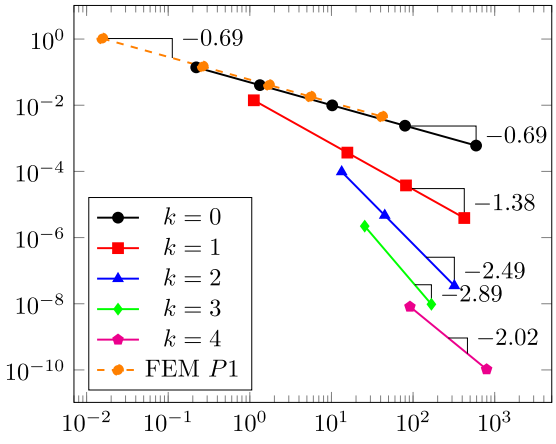

Fig. 5. $E - E_h$ versus total wall time in seconds.

only willing to invest in the solution a few seconds. We should also mention that the advantage is even bigger in practice given that, with high order, one uses less elements and, thus, also saves a lot of time by reducing the meshing time (which is not included in this analysis).

For the benchmark, we used tetrahedral meshes: on one hand, to be able to compare with the classical finite-element method and, on the other hand, because many efficient,

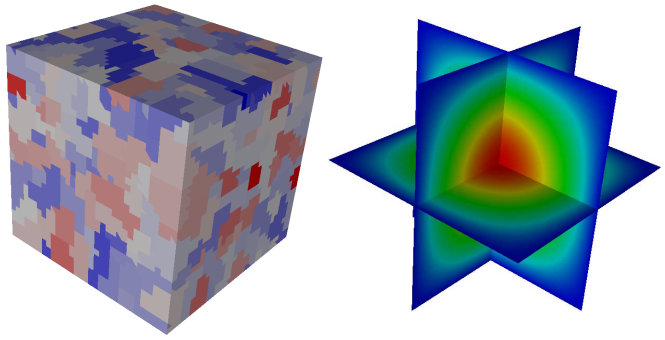

Fig. 6. Left: polyhedral mesh used in the computation composed by 470 polyhedral elements. Each different color represents a polyhedral mesh element obtained by gluing a set of tetrahedra belonging to a background mesh consisting of 270 000 tetrahedra. Right: result in terms of potential on three slices of the domain for $k = 1$.

automatic and open-source mesh generators for such elements exist and they are well integrated in the computer-assisted modeling chain. Moreover, the convergence slopes are correctly retrieved only if the set of meshes is produced by recursively subdividing the coarsest one. Now, this is quite difficult to perform with general polyhedral meshes, because the appropriate tools are currently still being developed.

To validate the method also with general polyhedral elements, we start from an initial mesh composed of tetrahedral elements which is fine enough to capture the geometric features of the domain (e.g., curved boundaries) and the scale of the exact solution. We then perform computations on a polyhedral mesh obtained by agglomerating elements of the background tetrahedral mesh. Doing so, we obtain, e.g., the mesh with 470 polyhedra, as represented in Fig. 6. The correct solution obtained with MHO and $k = 1$ is represented in Fig. 6. A similar technique has been used in the adaptive coarsening strategy [3], which is a new procedure that is able to drastically reduce the number of DOFs with respect to the ones resulting from the tetrahedral background mesh without the need to regenerate a new mesh.

REFERENCES

[1] L. Beirão da Veiga and A. Ern, "Preface to the special issue polyhedral discretization for PDE," *ESAIM: M2AN*, vol. 50, no. 3, pp. 633–634, 2016.

[2] L. Codecasa, R. Specogna, and F. Trevisan, "A new set of basis functions for the discrete geometric approach," *J. Comput. Phys.*, vol. 229, no. 19, pp. 7401–7410, 2010.

[3] D. A. Di Pietro and R. Specogna, "An a posteriori-driven adaptive mixed high-order method with application to electrostatics," *J. Comput. Phys.*, vol. 326, pp. 35–55, Dec. 2016.

[4] D. A. Di Pietro and A. Ern, "Arbitrary-order mixed methods for heterogeneous anisotropic diffusion on general meshes," *IMA J. Numer. Anal.*, vol. 37, no. 1, pp. 40–93, 2017.

[5] R. Specogna, "One stroke complementarity for poisson-like problems," *IEEE Trans. Magn.*, vol. 51, no. 3, Mar. 2015, Art. no. 7401404.

[6] D. A. Di Pietro and A. Ern, "Mathematical aspects of discontinuous Galerkin methods," in *Mathematics and Applications*. Berlin, Germany: Springer, 2012.

[7] J. Aghili, S. Boyaval, and D. A. Di Pietro, "Hybridization of mixed high-order methods on general meshes and application to the Stokes equations," *Comput. Meth. Appl. Math.*, vol. 15, no. 2, pp. 111–134, 2015.

[8] Y. Notay, "An aggregation-based algebraic multigrid method," *Electron. Trans. Numer. Anal.*, vol. 37, pp. 123–146, 2010.